BIOCHEMISTRY
including biophysical chemistry & molecular biology
Article

Biochemistry **2010,** *49,* 9391–9401 9391
DOI: 10.1021/bi1010688

A Conserved Glutamate Controls the Commitment to Acyl-Adenylate Formation in Asparagine Synthetase†

Megan E. Meyer,‡ Jemy A. Gutierrez,‡,§ Frank M. Raushel,‖ and Nigel G. J. Richards*,‡

‡*Department of Chemistry, University of Florida, P.O. Box 117200, Gainesville, Florida 32611, United States, and*
‖*Department of Chemistry, Texas A&M University, P.O. Box 30012, College Station, Texas 77843, United States*
§*Present address: Department of Biochemistry, Albert Einstein College of Medicine, 1300 Morris Park Ave., Bronx, NY 10461*

Received July 3, 2010; Revised Manuscript Received September 17, 2010

ABSTRACT: Inhibitor docking studies have implicated a conserved glutamate residue (Glu-348) as a general base in the synthetase active site of the enzyme asparagine synthetase B from *Escherichia coli* (AS-B). We now report steady-state kinetic, isotope transfer, and positional isotope exchange experiments for a series of site-directed AS-B mutants in which Glu-348 is substituted by conservative amino acid replacements. We find that formation of the β-aspartyl-AMP intermediate, and therefore the eventual production of asparagine, is dependent on the presence of a carboxylate side chain at this position in the synthetase active site. In addition, Glu-348 may also play a role in mediating the conformational changes needed to (i) coordinate, albeit weakly, the glutaminase and synthetase activities of the enzyme and (ii) establish the structural integrity of the intramolecular tunnel along which ammonia is translocated. The importance of Glu-348 in mediating acyl-adenylate formation contrasts with the functional role of the cognate residues in β-lactam synthetase (BLS) and carbapenam synthetase (CPS) (Tyr-348 and Tyr-345, respectively), which both likely evolved from asparagine synthetase. Given the similarity of the chemistry catalyzed by AS-B, BLS, and CPS, our work highlights the difficulty of predicting the functional outcome of single site mutations on enzymes that catalyze almost identical chemical transformations.

Human asparagine synthetase (hASNS)[1] catalyzes the ATP-dependent synthesis of L-asparagine from L-aspartic acid using L-glutamine as the nitrogen source (Scheme 1) (*1*). A number of observations make hASNS of interest as a drug target. For example, hASNS has been shown to be a predictive biomarker for ovarian cancer (*2*, *3*). Moreover, the constitutive expression of hASNS in transformed MOLT-4 cells permits them to grow in the presence of asparaginase (*4*), thereby supporting hypotheses concerning the role of hASNS in the molecular mechanisms that cause resistance to current clinical protocols for treating acute lymphoblastic leukemia (ALL) (*5*). The physiological importance of hASNS-mediated asparagine biosynthesis in both ovarian cancer and ALL is also supported by our recent finding that the adenylated sulfoximine **1** (Figure 1), which is the first inhibitor of hASNS with nanomolar potency, suppresses proliferation of an asparaginase-resistant MOLT-4 cell line (*6*).

Scheme 1: Overall Reaction Catalyzed by Glutamine-Dependent ASNS

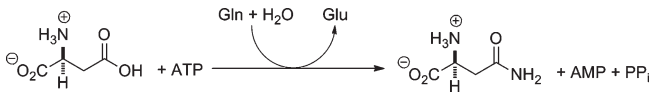

For a variety of technical reasons, in part associated with the need to employ baculovirus-based expression for preparing large amounts of recombinant, wild-type hASNS (*7*), almost all mechanistic and structural studies of the enzyme have been performed using the glutamine-dependent asparagine synthetase present in *Escherichia coli* (AS-B) (*8*−*11*). In an important development for structure-based discovery of new hASNS inhibitors with improved activity in cell-based assays (*12*), our group was able to obtain a high-resolution crystal structure for the C1A AS-B mutant (in which Cys-1 is replaced by an alanine residue) complexed to L-glutamine and AMP (Figure 1A) (*13*). The adenylated sulfoximine **1** also inhibits AS-B (*14*), presumably by forming similar intermolecular interactions given that residues within the synthetase active sites of hASNS and AS-B are completely conserved. Using homology modeling methods (*15*, *16*), we have been able to develop a computational model of the hASNS inhibitor **1** bound within the AS-B synthetase site (Figure 1B) and are systematically validating this model of the AS-B/sulfoximine complex.[2] For example, recent work has confirmed that the electrostatic interaction between the phosphate moiety in **1** and the side chain of a conserved active

†This work was supported by the Chiles Endowment Biomedical Research Program of the Florida Department of Health (N.G.J.R.) and the National Institutes of Health (Grant DK30343 to F.M.R.). Funding for a predoctoral studentship (M.E.M.) from an NIH training grant in Cancer Biology (CA09126) is also gratefully acknowledged.

*To whom correspondence should be addressed: 352-392-3601 (office); 352-846-2095 (fax); richards@qtp.ufl.edu (e-mail).

[1]Abbreviations: hASNS, human asparagine synthetase; ALL, acute lymphoblastic leukemia; AS-B, *Escherichia coli* asparagine synthetase B; AMP, adenosine 5′-monophosphate; βAspAMP, β-aspartyl-AMP; DNFB, 2,4-dinitrofluorobenzene; DTT, dithiothreitol; EPPS, 3-[4-(2-hydroxyethyl)-1-piperazinyl]propanesulfonic acid; PP_i, inorganic pyrophosphate; LC-ESI, liquid chromatography−electrospray ionization; WT, wild type; PIX, positional isotope exchange; BLS, β-lactam synthetase; CPS, carbapenam synthetase; GMPS, guanosine 5′-monophosphate synthetase; ASNS, glutamine-dependent asparagine synthetase.

[2]Y. Ding, R. N. Humkey, and N. G. J. Richards, to be published. Coordinate data for the model complex are available on request.

Published on Web 09/20/2010

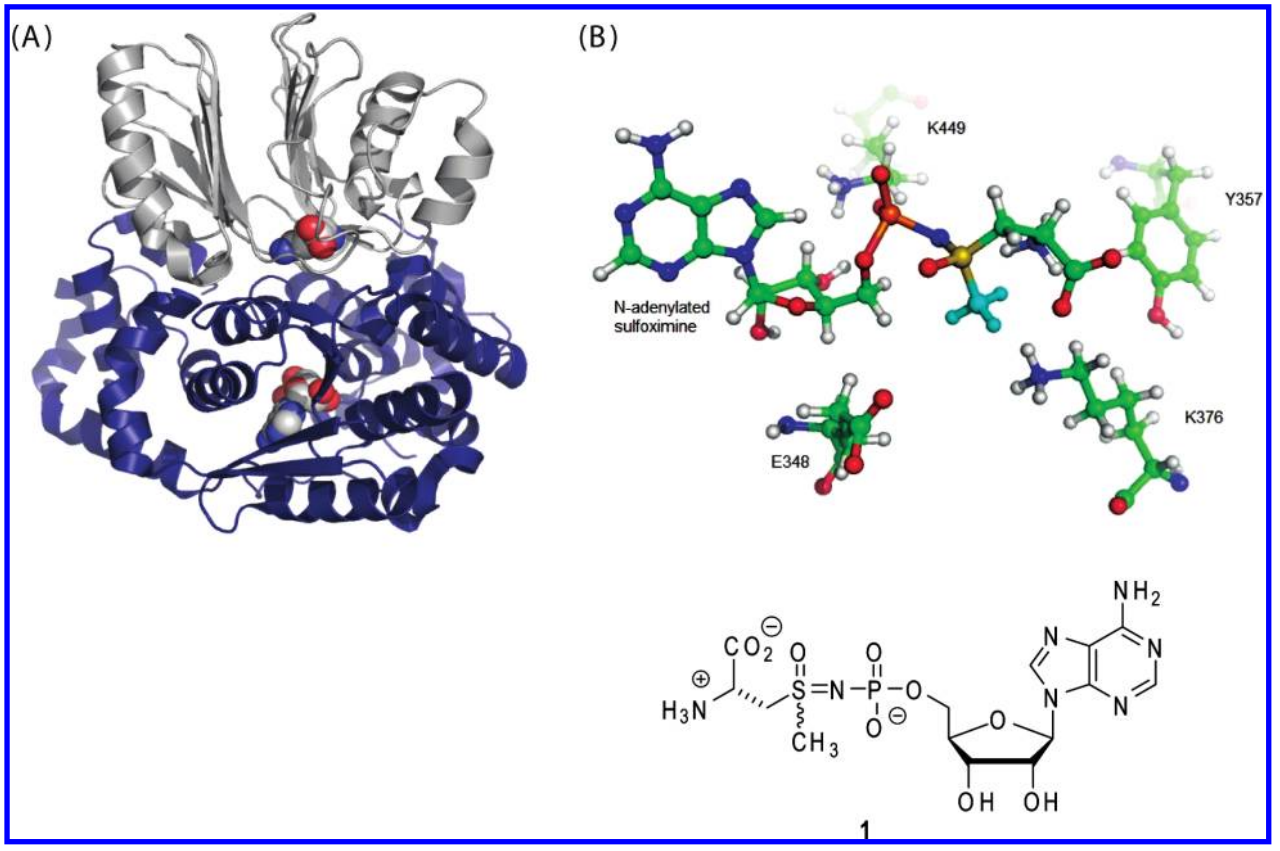

FIGURE 1: (A) Cartoon representation of the *E. coli* AS-B C1A mutant complexed to glutamine and AMP (1CT9) (*14*). The N-terminal glutaminase and C-terminal synthetase domains of each monomer are colored gray and blue, respectively. Bound glutamine (top) and AMP (bottom) are shown as CPK models. (B) Computational model for inhibitor **1** bound within the synthetase active site of AS-B, indicating the possible proximity of the Glu-348 side chain carboxylate and the electron-deficient methyl group (cyan) in the N-adenylated sulfoximine that mimics ammonia. Coloring: C, gray; H, white; O, red; N, blue; S, yellow; P, orange. Both images were rendered in PYMOL (DeLano Scientific Software LLC, Palo Alto, CA).

site lysine residue (Lys-449 in AS-B) is critical for inhibitor binding (*17*).

Despite this initial success in validating our model for how the adenylated sulfoximine might bind to the synthetase site, we are undertaking a series of systematic studies to test other predictions of the computational structure. For example, simple modeling suggested that the Glu-348 side chain could be positioned close to the methyl group of sulfoximine **1**, a moiety thought to mimic an ammonia molecule in the transition state undergoing nucleophilic attack on a β-aspartyl-AMP intermediate **2** (βAspAMP) (*6*), which is tightly bound by the enzyme (*8*, *18*, *19*). We now report the results of efforts to ascertain the functional role of Glu-348 in catalysis, which have sought to confirm the possibility that Glu-348 functions as a general base to facilitate nucleophilic attack of enzyme-bound ammonia on βAspAMP (Scheme 2). Somewhat unexpectedly, this work implicates Glu-348 in mediating βAspAMP formation and suggests that this conserved residue may also participate in the molecular mechanisms coordinating catalytic activity in the weakly coupled glutaminase and synthetase sites of the enzyme.

MATERIALS AND METHODS

General. Unless otherwise stated, all chemicals were purchased from Sigma (St. Louis, MO) or Fischer Scientific (Pittsburgh, PA) and were of the highest available purity. L-Glutamine was recrystallized prior to use, as previously described (*8*). Protein concentrations were determined using the Bradford assay (Pierce, Rockford, IL) (*20*) and corrected as previously described (*18*). All DNA primers were obtained from Integrated DNA Technologies, Inc. (Coralville, IA), and DNA sequencing was performed by the core facility in the Interdisciplinary Center for Biotechnology Research at the University of Florida. 2,4-Dinitrofluorobenzene (DNFB) was obtained from Aldrich (St. Louis, MO). ***Caution***: Extreme care should be taken when handling solutions of DNFB in organic solvents because this reagent is a potent allergen and will penetrate many types of laboratory gloves (*21*).

Expression and Purification of C-Terminally Tagged AS-B and AS-B Mutants. The *asnB* gene encoding AS-B was cloned into the pET-21c(+) plasmid (Novagen, Madison, WI) and expressed following literature procedures (*22*). Site-directed mutagenesis to obtain genes encoding AS-B mutants was performed using the QuikChange kit (Stratagene, La Jolla, CA) using standard primers. After expression of the C-terminally tagged AS-B or AS-B mutant, the cellular pellet was resuspended in 50 mM EPPS, pH 8, containing 300 mM NaCl, 10 mM imidazole, 1% Triton X, and 0.5 mM DTT (50 mL) before sonication. Cellular debris was removed by centrifugation (10000*g*, 20 min, 4 °C), and the resulting supernatant was loaded onto a Ni-NTA column (Qiagen, Valencia, CA). This column was then washed with 50 mM EPPS, pH 8.0, containing 300 mM NaCl, 20 mM imidazole, and 0.5 mM DTT (5 × 3 mL) before the His_6-tagged AS-B or AS-B mutant was eluted with 50 mM EPPS, pH 8.0, containing 300 mM NaCl, 250 mM imidazole, and 0.5 mM DTT (10 × 3 mL). Fractions containing enzyme were identified using SDS−PAGE, pooled, and dialyzed against 50 mM EPPS, pH 8.0, containing 5 mM DTT. Glycerol was

Scheme 2: Reactions Catalyzed in the Synthetase Active Site of Glutamine-Dependent ASNS Showing the Structure of the βAs-pAMP Intermediate **2** and the Transition State for the Subsequent Attack of Ammonia To Form Asparagine and AMP

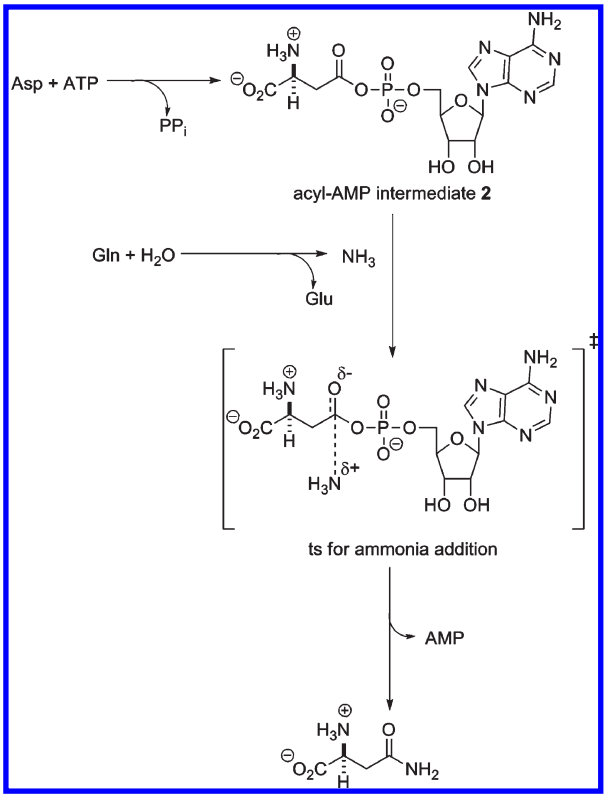

added (to a final concentration of 20%) to the dialyzed enzyme (approximately 1 mg/mL), and aliquots were stored at −80 °C.

Steady-State Kinetic Assays. Synthetase activity was assayed by monitoring the production of inorganic pyrophosphate (PP_i) spectrophotometrically using a standard coupled enzyme assay (Sigma Technical Bulletin BI-100) (*10*).[3] Assay mixtures consisted of 5 mM ATP, 20 mM L-aspartic acid, and PP_i assay reagent (350 μL) dissolved in 100 mM EPPS, pH 8.0, containing 10 mM $MgCl_2$ and either 20 mM L-glutamine or 100 mM NH_4Cl as a nitrogen source (1 mL total volume). Reaction was initiated by the addition of enzyme (2−4 μg), and PP_i formation was determined over a period of 20 min at 37 °C by monitoring the change in absorbance at 340 nm. In experiments to determine steady-state kinetic parameters, the initial concentration of either ATP (0−3 mM) or L-aspartic acid (0−10 mM) was varied while maintaining the other substrates at the levels outlined above. Measurements were made at specific substrate and enzyme concentrations in triplicate, and data were analyzed to obtain the values of V and V/K using standard computer-based methods (*23*).

The determination of the glutaminase activity exhibited by the C-terminally tagged AS-B and AS-B mutants was performed using standard procedures (*22*). Hence, the enzyme (1.5 μg) was incubated in the presence, or absence, of 5 mM ATP with L-glutamine (0.2−50 mM) in 100 mM EPPS, pH 8.0, containing 100 mM NaCl and 8 mM $MgCl_2$ (200 μL total volume) for 20 min at 37 °C. The glutaminase reaction was then quenched by the addition of trichloroacetic acid, to a final concentration of 4%, and the resulting solution was added to 300 mM glycine/250 mM hydrazine buffer, pH 9.0, containing 1.5 mM NAD^+ and 1 mM ADP. L-Glutamate dehydrogenase (2.5 units) (Sigma, St. Louis, MO) was then added (final volume 500 μL), and the absorbance of the solution at 340 nm was taken after 30 min incubation at room temperature. The amount of L-glutamate was then quantified using a standard curve. Measurements were made at specific substrate and enzyme concentrations in triplicate, and data were analyzed to obtain the values of V and V/K using standard computer-based methods (*23*).

The ratio of L-asparagine and L-glutamate formed in the synthetase reaction was determined independently by monitoring peaks associated with both amino acids in a published HPLC-based assay (*18*, *24*). Hence, reaction mixtures containing enzyme (2−4 μg), 5 mM ATP, 10 mM L-aspartic acid, and either 100 mM NH_4Cl or 20 mM L-glutamine dissolved in 100 mM EPPS, pH 8.0, containing 10 mM $MgCl_2$ (1 mL total volume) were incubated for 20 min at 37 °C. Reactions were initiated by the addition of AS-B, or the appropriate AS-B mutant, and quenched using glacial AcOH (4%) to precipitate the enzyme. The solution was then neutralized using 10 M NaOH, and an aliquot (40 μL) was mixed with 400 mM Na_2CO_3 buffer (80 μL), pH 9, DMSO (20 μL), and a saturated solution of DNFB in absolute EtOH (60 μL). The resulting solution was heated at 50 °C for 50 min before being cooled and quenched with glacial AcOH (40 μL). The mixture was then analyzed by reverse-phase HPLC using a Varian Microsorb C_{18} column. The derivatized amino acids were eluted using a step gradient of 40 mM formic acid buffer, pH 3.6, and CH_3CN, such that the initial CH_3CN concentration was 14%. After 30 min the amount of CH_3CN was increased to 20% over a period of 30 s, and elution continued for an additional 10 min. 2,4-Dinitrobenzene-tagged asparagine and glutamate were detected by UV (365 nm) and quantified by comparison to authentic standards (Sigma, St. Louis, MO).

Preparation of [^{18}O]Aspartic Acid and [β,γ-$^{18}O_6$]ATP. [^{18}O]-L-Aspartic acid was prepared by incubating the unlabeled amino acid in 95% $H_2{}^{18}O$ under acidic conditions for 14 days, as outlined previously (*8*). The final reaction mixture was lyophilized, [^{18}O]aspartic acid was dissolved in water to a final concentration of 2.1 M, and the solution pH was adjusted to 8 using 10 M NaOH. The extent of ^{18}O labeling was determined by isocratic C_{18} LC-ESI mass spectrometry in negative ion mode (Thermo-Finnigan LCQ). ^{18}O-Labeled ATP was prepared from ^{18}O-labeled carbamoyl phosphate,[4] AMP, a trace of ATP, adenylate kinase, and carbamate kinase as described previously (*25*), with minor modifications to the literature procedure (*26*). Integration of the ^{31}P signals associated with the β- and γ-phosphate atoms in the ^{18}O-labeled ATP indicated that the average level of isotope incorporation was 75%.

Isotope (^{18}O) Transfer Experiments. Reaction mixtures were prepared containing 100 mM NH_4Cl, 10 mM ATP, 20 mM $MgCl_2$, and 20 mM [^{18}O]aspartic acid dissolved in 100 mM EPPS, pH 8.0 (1 mL total volume). Asparagine synthesis was initiated by addition of AS-B (200 μg), and the reaction mixture was incubated for 3 h at 37 °C before being quenched with trichloroacetic acid (4% final concentration). After enzyme precipitation by centrifugation, the supernatant (700 μL) was

[3]This assay is composed of the enzymes pyrophosphate-dependent fructose-6-phosphate kinase, aldolase, triose phosphate isomerase, and glycerophosphate dehydrogenase. Pyrophosphate production is therefore measured by monitoring the oxidation of NADH spectroscopically at 340 nm.

[4]The sample of isotopically labeled carbamoyl phosphate contained four ^{18}O atoms bonded to phosphorus (*26*).

Table 1: Steady-State Kinetic Parameters for the Glutaminase Activity of C-Terminally Tagged AS-B and the Site-Specific AS-B Mutants[a]

	ATP absent			5 mM ATP present		
enzyme	K_m (mM)	k_{cat} (s^{-1})	k_{cat}/K_m (M^{-1} s^{-1})	K_m (mM)	k_{cat} (s^{-1})	k_{cat}/K_m (M^{-1} s^{-1})
WT AS-B	5.0 ± 1.4 (1.67)[b]	6.2 ± 0.2 (3.38)	1190 (2020)	1.7 ± 0.5 (1.30)	6.6 ± 0.1 (5.91)	3880 (4540)
E348D	2.7 ± 0.4	4.1 ± 0.1	1510	1.1 ± 0.2	10.02 ± 0.07	9100
E348A	5.8 ± 0.8	6.37 ± 0.04	1100	3.5 ± 0.7	5.8 ± 0.2	1660
E348Q	9 ± 4	4.0 ± 0.5	450	3.9 ± 0.3	4.45 ± 0.07	1140

[a]Reaction mixtures of enzyme (1.5 μg) and L-glutamine (0.2−50 mM) dissolved in 100 mM EPPS, pH 8.0, containing 100 mM NaCl and 10 mM $MgCl_2$ (200 μL total volume) were incubated, in the presence or absence of 5 mM ATP, for 20 min at 37 °C. Glutamate was quantified using glutamate dehydrogenase (*22*). [b]Values shown in parentheses are literature values reported previously for recombinant, untagged WT AS-B (*18*).

Table 2: Steady-State Kinetic Parameters for the Synthetase Activity of C-Terminally Tagged AS-B and the E348D AS-B Variant[a]

	ATP			aspartate		
enzyme	$K_{m(app)}$ (mM)	k_{cat} (s^{-1})	$k_{cat}/K_{m(app)}$ (M^{-1} s^{-1})	$K_{m(app)}$ (mM)	k_{cat} (s^{-1})	$k_{cat}/K_{m(app)}$ (M^{-1} s^{-1})
			Glutamine-Dependent Activity			
WT AS-B	0.10 ± 0.01 (0.26)[b]	0.90 ± 0.01 (2.18)[b]	9000 (8380)[b]	0.58 ± 0.04 (0.85)[b]	0.67 ± 0.02 (1.56)[b]	1200 (1830)[b]
E348D	0.013 ± 0.004	0.51 ± 0.02	39200	0.13 ± 0.01	0.45 ± 0.01	3450
			Ammonia-Dependent Activity			
WT AS-B	0.11 ± 0.03	0.96 ± 0.02	8700	1.2 ± 0.1 (0.53)[c]	0.75 ± 0.03 (1.09)[c]	630 (800)[c]
E348D	0.03 ± 0.01	0.43 ± 0.03	14300	0.23 ± 0.07	0.30 ± 0.02	1300

[a]All measurements were performed at pH 8. Assay mixtures consisted of enzyme (2−4 μg), PP_i assay reagent (350 μL), and either 20 mM L-glutamine or 100 mM NH_4Cl dissolved in 100 mM EPPS containing 10 mM $MgCl_2$ (1 mL total volume). Assay mixtures were augmented with 20 mM L-aspartic acid and ATP (0−3 mM) or 5 mM ATP and aspartic acid (0−10 mM) when determining steady-state parameters for ATP and L-aspartic acid, respectively. [b]Values shown in parentheses are literature values reported previously for untagged WT AS-B (*18*). [c]Values shown in parentheses are literature values reported previously for untagged WT AS-B (*30*) although the published values of k_{cat} have been corrected by a factor of 2.73 for reasons discussed elsewhere (*8*).

transferred to a new tube containing EDTA (0.0287 g), glycine (0.045 g), and D_2O (200 μL). The pH was adjusted to 9.5 using 10 M NaOH, and an aliquot was transferred to an NMR tube (800 μL). ^{31}P NMR spectra were recorded at 121 MHz with broad-band proton decoupling on a Mercury 300 spectrometer, at a sample temperature of 23 °C. Spectra were obtained from 500 scans with an acquisition time of 4.0 s. ^{31}P chemical shifts were referenced to 85% phosphoric acid.

Positional Isotope Exchange (PIX) Experiments. Positional isotope exchange was examined by ascertaining the extent of ^{18}O incorporation from [β,γ-$^{18}O_6$]ATP as a function of time (*28*). Assay mixtures contained 5 mM [β,γ-$^{18}O_6$]ATP, 10 mM L-Asp, and 10 mM $MgCl_2$ dissolved in 100 mM EPPS, pH 8.0, with the appropriate enzyme (3 μM AS-B, 3 μM E348D, 3 μM E348A) (4 mL total volume). Reactions were incubated at 37 °C and aliquots (500 μL) removed at 30 min intervals, which were then quenched by the addition of 1.0 M EDTA (125 μL) and D_2O (125 μL) before being transferred to an NMR tube. Control experiments confirmed that these samples contained sufficient EDTA to chelate all of the Mg^{2+} ions required for reaction. ^{31}P NMR spectra were recorded at 121 MHz with broad-band proton decoupling on a Mercury 300 spectrometer, at a sample temperature of 23 °C. Spectra were obtained from 3000 scans with an acquisition time of 4.0 s. ^{31}P chemical shifts were referenced to 85% phosphoric acid.

RESULTS AND DISCUSSION

Expression, Purification, and Characterization of C-Terminally His_6-Tagged AS-B. Early efforts to characterize the functional role of Glu-348 in untagged, recombinant WT AS-B revealed the presence of a contaminating ATPase activity in preparations of the E348A AS-B mutant, where Glu-348 is replaced by alanine. A similar contaminating activity was reported in samples of hASNS obtained from a yeast-based expression system (*29*), which was eventually identified as being associated with the presence of a DNA damage-responsive protein (*30*). In an effort to determine whether we had unmasked an intrinsic ATPase activity associated with the synthetase site of the E348A AS-B mutant or were merely observing an impurity in the recombinant enzyme, we expressed and purified an AS-B variant containing a C-terminal polyhistidine (His_6) tag. As observed for human ASNS (*7*), steady-state assays showed that the presence of the purification tag did not greatly perturb the steady-state kinetic parameters for glutaminase activity compared to that of untagged AS-B (Table 1). In addition, the presence of 5 mM ATP in the assay gave a 3-fold increase in the specificity constant k_{cat}/K_m for the tagged enzyme (Table 1), consistent with previous observations on untagged AS-B (*22*, *31*). An approximately 2-fold decrease in k_{cat} was observed for both the glutamine- and ammonia-dependent synthetase activities of C-terminally tagged AS-B (Table 2). These small changes in activity are also reflected by the approximately 7.2:1 Glu:Asn ratio observed when the C-terminally tagged enzyme is incubated with saturating concentrations of all substrates (Table 3) rather than the 1.8:1 Glu:Asn ratio reported for untagged AS-B under identical conditions (*18*). We note that the concentration of asparagine and glutamate formed under the reaction conditions was measured directly using an HPLC-based assay (*18*, *24*). In light of the fact that k_{cat}/K_m values of the glutaminase and synthetase activities were little changed by the presence of the C-terminal His_6 motif, all of the AS-B mutants used to delineate

Table 3: Product Stoichiometry for the Glutamine-Dependent Synthetase Activity of C-Terminally Tagged AS-B and the E348D AS-B Mutant[a]

enzyme	μmol of Asn min^{-1} mg^{-1}	μmol of Glu min^{-1} mg^{-1}	Glu:Asn
WT AS-B	0.64 ± 0.04	4.6 ± 0.2	7.2:1
E348D	0.36 ± 0.04	6.5 ± 0.7[b]	18:1

[a]Reaction mixtures containing enzyme (2−4 μg), 5 mM ATP, 10 mM L-aspartic acid, and 20 mM L-glutamine dissolved in 100 mM EPPS, pH 8.0, containing 10 mM $MgCl_2$ (1 mL total volume) were incubated for 20 min at 37 °C. Amino acids were derivatized and quantitated by HPLC using a published procedure (*18*). [b]Although the E348A and E348Q AS-B mutants did not synthesize asparagine under these conditions, they did exhibit glutaminase activity and formed glutamate at rates of 2.8 ± 0.3 μmol of Glu min^{-1} mg^{-1} and 4.1 ± 0.4 μmol of Glu min^{-1} mg^{-1}, respectively.

Table 4: Product Stoichiometry for the Ammonia-Dependent Synthetase Activity of C-Terminally Tagged AS-B and the E348D AS-B Mutant[a]

enzyme	μmol of Asn min^{-1} mg^{1}	μmol of PP_i min^{-1} mg^{-1}	PP_i:Asn
WT AS-B	0.63 ± 0.03	0.59 ± 0.05	1:1
E348D	0.33 ± 0.01	0.33 ± 0.06[b]	1:1

[a]Reaction mixtures containing enzyme (2−4 μg), 5 mM ATP, 10 mM L-aspartic acid, and 100 mM NH_4Cl dissolved in 100 mM EPPS, pH 8.0, containing 10 mM $MgCl_2$ (1 mL total volume) were incubated for 20 min at 37 °C. Amino acids were derivatized and quantitated by HPLC using a published procedure (*18*). [b]Although the E348A and E348Q AS-B mutants did not synthesize asparagine under these conditions, they did exhibit a low level of ATPase activity and formed inorganic pyrophosphate at rates of 0.04 ± 0.01 μmol of PP_i min^{-1} mg^{-1} and 0.07 ± 0.01 μmol of PP_i min^{-1} mg^{-1}, respectively.

the functional role of Glu-348 were expressed so that the C-terminal His_6 tag was present and purified using a Ni-NTA column.

Steady-State Kinetic Characterization of the C-Terminally His_6-Tagged E348A, E348D, and E348Q AS-B Mutants. Although all of the three AS-B mutants exhibited similar glutaminase activity to the WT enzyme in the absence of ATP (Table 1), only the E348D AS-B mutant was capable of catalyzing asparagine formation when glutamine was employed as a nitrogen source (Table 2). Thus, no synthetase activity could be observed for the E348A and E348Q mutants even using a sensitive HPLC-based assay. Given that substitution of Glu-348 might have affected the structure of the protein, we evaluated the effect of ATP on the glutaminase activities of the three AS-B mutants. Perhaps surprisingly, the glutaminase activity of the E348D AS-B mutant was stimulated more than 6-fold relative to WT AS-B by the presence of 5 mM ATP (Table 1), suggesting that any intramolecular interactions involved in coordinating catalysis at the two active sites might have been affected by the altered size of the side chain. In contrast, ATP-dependent stimulation of glutaminase activity in the E348A and E348Q AS-B mutants was less than that of WT enzyme, with only a 2-fold increase seen for the E348Q AS-B mutant (Table 1). Taken overall, these results supported the hypothesis that Glu-348 was functionally important, consistent with the predictions of our model for the AS-B/sulfoximine complex.

Using direct measurements of glutamate, asparagine, and PP_i formation, we next examined whether replacing Glu-348 by aspartate might give rise to "uncoupled" product stoichiometries. Both WT AS-B and the E348D AS-B mutant formed pyrophosphate and asparagine in a 1:1 ratio when all substrates were present (Table 4). In an unexpected observation, the E348A and E348Q AS-B mutants were also able to form PP_i under these reaction conditions (Figure 2A) despite being unable to catalyze asparagine formation, at least at the detection limits of our sensitive HPLC-based assay (*18*). Hence, these two AS-B mutants either possessed an intrinsic ATPase activity or were unable to catalyze the addition of ammonia to the βAspAMP intermediate. Similar findings were made when the nitrogen source was ammonia rather than L-glutamine (Figure 2B). The rate of pyrophosphate production for WT AS-B and the three AS-B mutants was therefore remeasured in assay mixtures from which aspartate was absent, i.e., in the presence of only $MgCl_2$, glutamine, and ATP. These experiments revealed that AS-B did seem to exhibit an intrinsic ability to catalyze the conversion of ATP into AMP and PP_i in the presence of a nitrogen source that was 10% (or less) of the synthetase activity when aspartate was omitted from the reaction mixture (Figure 2). Given the new

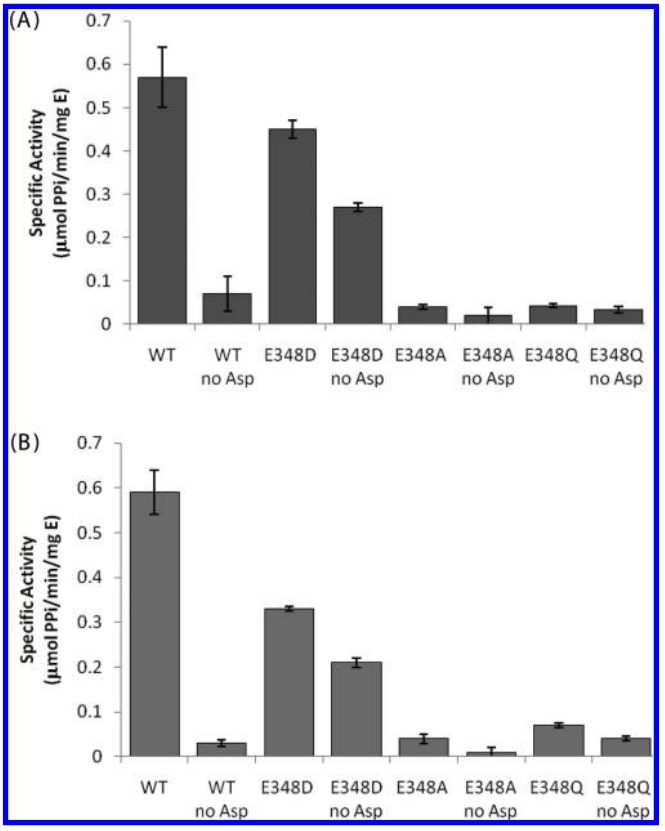

FIGURE 2: Specific activities of PP_i formation in the presence and absence of aspartate for the (A) glutamine-dependent and (B) ammonia-dependent reactions of WT AS-B and the three E348 mutants.

purification methodology, we attributed this activity to AS-B itself rather than any contaminant, a hypothesis that is supported by the fact that the E348D AS-B mutant converted ATP to AMP and PP_i in the absence of aspartate at a rate that was approximately 60% of that seen for asparagine production. Given that the Asn:PPi ratio was 1:1 (at least within the limits of our assays) for both WT AS-B and the E348D AS-B mutant when all substrates are present in the reaction mixture, it seems that aspartate acts to suppress this intrinsic ATPase activity, perhaps through a conformational change that prevents water from entering the synthetase active site or by ensuring that ATP is bound within the enzyme so as to preclude its hydrolysis. Finally, the presence of aspartate did not affect the low rate of ATP breakdown catalyzed by the E348A and E348Q AS-B mutants to any significant extent under these reaction conditions, which was taken as evidence for the idea that these two mutants were incapable of catalyzing the formation of βAspAMP.

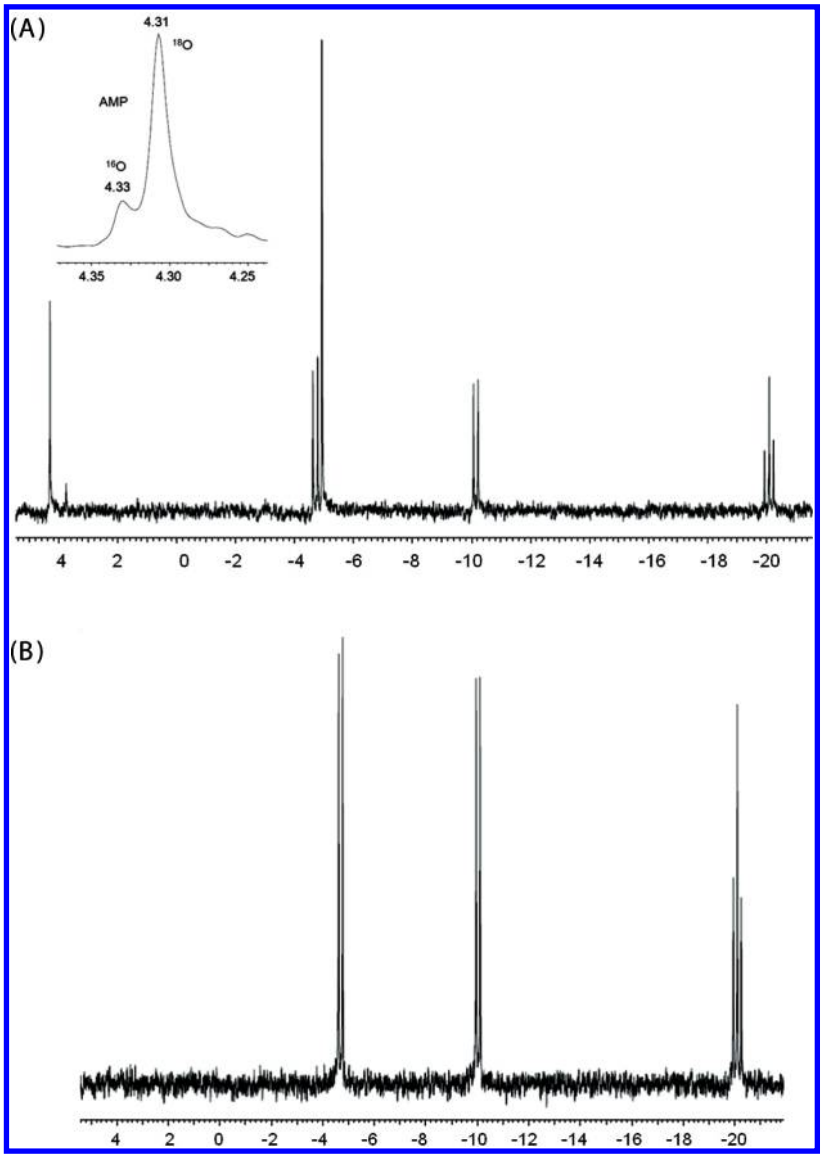

FIGURE 3: (A) ^{31}P NMR spectrum of the reaction mixture containing ATP, NH_4Cl, $MgCl_2$, ^{18}O-labeled aspartate, and the E348D AS-B mutant in EPPS, pH 8 (full details are provided in Materials and Methods). Peaks for ^{18}O- and ^{16}O-labeled AMP are separated by 0.02 ppm (inset). No ^{18}O-labeled PP_i was observed. (B) ^{31}P NMR spectrum of the reaction mixture containing ATP, NH_4Cl, $MgCl_2$, ^{18}O-labeled aspartate, and the E348A AS-B mutant in EPPS, pH 8 (full details are provided in Materials and Methods). No NMR detectable amounts of either AMP or PP_i were produced under these conditions. ^{31}P chemical shifts are referenced to 85% phosphoric acid.

Another interesting finding in these studies of product stoichiometry was that the Glu:Asn ratio for the E348D AS-B mutant increased to a value of 18:1; i.e., the glutaminase and synthetase activities had become more uncoupled than those of the wild-type enzyme (7.2:1 ratio) (Table 3). This observation is consistent with the hypothesis that Glu-348 plays a role in facilitating the attack of ammonia on the βAspAMP intermediate, perhaps by acting as a general base. On the other hand, the inability of the E348A and E348Q AS-B mutants to produce asparagine even though their glutaminase activities were similar to that of the wild-type enzyme suggested that the side chain of Glu-348 might have another function in catalysis.

Steady-state kinetic parameters were determined for the synthetase reaction catalyzed by the E348D mutant in an effort to delineate the functional role of Glu-348 (Table 2). A 5-fold decrease in the $K_{m(app)}$ value for aspartate was observed for both the glutamine- and ammonia-dependent synthetase reactions, together with a k_{cat} that was half of that observed for the wild-type enzyme, as measured by PP_i production (Table 2). The latter value is consistent with the relative rates of asparagine production measured by HPLC for the two enzymes when all substrates are present at saturating concentrations (Table 3). As a result of these altered steady-state parameters, $k_{cat}/K_{m(app)}$ for aspartate was increased almost 3-fold for the E348D AS-B mutant when glutamine was the nitrogen source. When ammonia was used in these assays, a 2-fold increase in $k_{cat}/K_{m(app)}$ for aspartate was observed. The steady-state parameters for ATP also exhibited similar changes for the E348D AS-B mutant independent of the nitrogen source. Given that both k_{cat} and $K_{m(app)}$ were decreased for both substrates in the glutamine-dependent synthetase reaction, it was possible that the mutation was slowing the formation rate of βAspAMP relative to the rate of breakdown, which would not be anticipated if ammonia addition to the intermediate was being impaired by the shorter side chain in the E348D AS-B mutant. In turn, this implied that the inability of the E348A and E348Q AS-B mutants to form asparagine might be associated with problems in forming the βAspAMP intermediate rather than with enzyme-facilitated ammonia attack to form asparagine and AMP.

Scheme 3: Schematic Representation of the Possible Outcomes of the ^{18}O PIX Experiment If Acyl-Adenylation Is Reversible and the PP_i Formed Can Undergo Rotation or "Flipping" within the Synthetase Active Site (*25*)

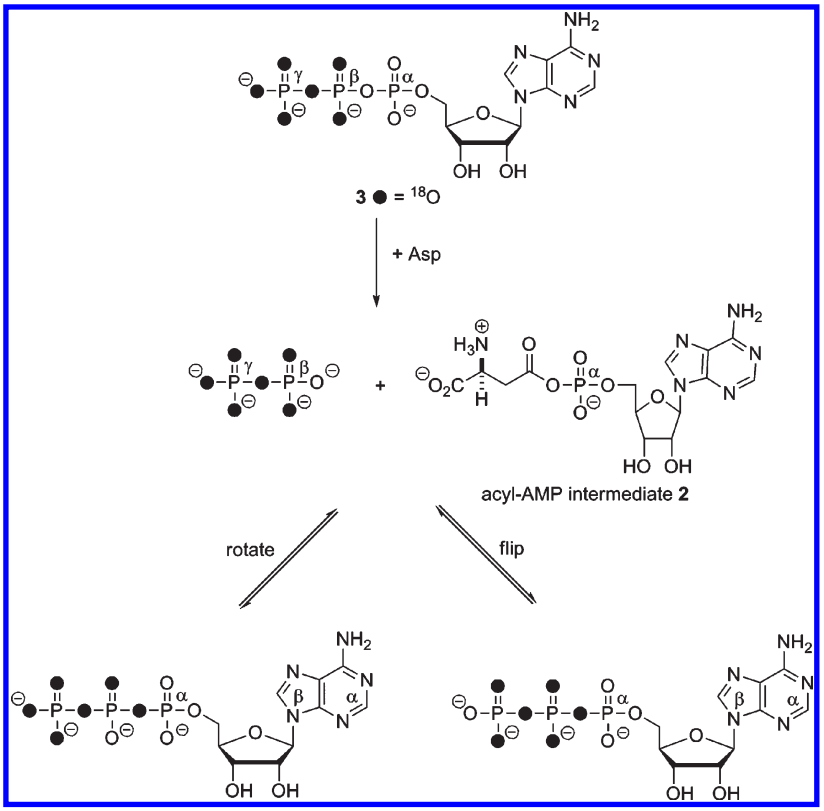

^{18}O Isotope Transfer Experiments. ^{31}P NMR-based assays were therefore undertaken to resolve the question of whether the βAspAMP intermediate was being formed by the E348A AS-B mutant. Thus, when His_6-tagged WT AS-B was incubated with ^{18}O-labeled aspartic acid, ATP, $MgCl_2$, and NH_4Cl in EPPS buffer, pH 8, the ^{31}P NMR spectrum showed signals from unreacted ATP, PP_i (δ 15.11 ppm), and two peaks for the ^{31}P nucleus in AMP separated by 0.02 ppm, providing clear evidence for the incorporation of ^{18}O into AMP and hence confirming formation of the βAspAMP intermediate (*8*, *26*, *27*, *32*). The addition of unlabeled AMP into the sample confirmed the assignment of the AMP peak. Similarly, incubation of the E348D AS-B mutant with ^{18}O-labeled aspartic acid under identical conditions showed clear evidence for ^{18}O incorporation into AMP, again showing that this mutant was capable of catalyzing the formation of βAspAMP (Figure 3A). We note that the amounts of AMP and PP_i relative to unreacted ATP were lower, consistent with the reduced synthetase activity of the E348D AS-B mutant. In contrast, incubation of the E348A AS-B mutant under identical conditions gave a mixture for which the ^{31}P NMR spectrum only contained peaks from nuclei in unreacted ATP (Figure 3B). Hence, no detectable levels of AMP and PP_i were produced by these mutant enzymes, providing further support for the idea that Glu-348 plays an important role in catalyzing βAspAMP formation. Given that replacement of Glu-348 by alanine or glutamine might have altered the "on-enzyme" equilibrium constant for βAspAMP formation but that this intermediate was still being produced in a reversible addition reaction, positional isotope exchange experiments were undertaken to investigate this possibility (*28*).

Positional Isotope Exchange (PIX) Experiments. In earlier efforts to resolve the complicated kinetic mechanism of AS-B (*18*) βAspAMP formation in the synthetase active site was assumed to be irreversible, despite conflicting reports concerning the absence of ATP/PP_i exchange reported in early work on ASNS from various sources (*8*, *33*). Furthermore, when incubated with ATP and aspartic acid in the absence of a nitrogen source, AS-B exhibits burst kinetics on the basis of either AMP or PP_i production, ruling out the possibility that all substrates must be present before βAspAMP can be formed on the enzyme (*8*, *12*). Our PIX investigation afforded an opportunity to evaluate the reversibility of βAspAMP intermediate formation in WT AS-B because acyl-adenylate formation is accompanied by the release of ^{18}O-labeled PP_i when the enzyme is incubated with [β,γ-$^{18}O_6$]ATP **3** (Scheme 3). As a result, the ^{18}O labels in this enzyme-bound reaction product can scramble their positions, either by rotation or by "flipping" within the active site. In the event that the adenylation reaction is reversible, there is a 67% chance that an ^{18}O label is incorporated into the oxygen bridging the α- and β-phosphorus atoms in the regenerated ATP (Scheme 3). Similarly, if PP_i can "flip" within, or dissociate and rebind to, the synthetase active site, then an ^{18}O label will be transferred to the α,β bridging position with concomitant transfer of a ^{16}O isotope to the γ-phosphorus. Clearly, a combination of rotation and flipping events is possible, leading to a mixture of differentially ^{18}O-labeled ATP isotopomers. These changes can be followed by monitoring the chemical shift changes in the ^{31}P NMR of the nuclei in the ^{18}O-labeled ATP present in the assay mixture (*26*).

His_6-tagged WT AS-B was incubated with aspartate and [β,γ-$^{18}O_6$]ATP **3** (*25*) *in the absence of* either glutamine or ammonia. These conditions were chosen to minimize any forward commitment of the βAspAMP intermediate arising from reaction with ammonia in the active site, which would diminish the extent of PIX. However, no changes in the ^{31}P signals for the α- and γ-phosphorus peaks of ATP were observed under these

conditions over a period of 3.5 h (Figure 4A), setting an upper limit of 0.003 s^{-1} for PIX. In addition, ^{31}P resonances associated with AMP and PP_i were not observed in our NMR spectra (Figure S1; see Supporting Information), which was somewhat surprising given the low intrinsic ATPase activity observed for WT AS-B in the absence of aspartate (Figure 2).

The upper limit of 0.003 s^{-1} for PIX in C-terminally tagged WT AS-B is consistent with prior observations on argininosuccinate synthetase (*34*), another enzyme that forms an adenylated intermediate in the absence of aspartate (*35*), and in which the catalytic domain has the same three-dimensional fold as the C-terminal domain of AS-B (Figure S2; see Supporting Information) (*36*). Indeed, AS-B and argininosuccinate synthetase are only two members of a large group of enzymes that form adenylated intermediates and possess this domain fold (identified by an SGGDXS loop motif, where X is a hydrophobic residue (Figure 5) (*37*)), including β-lactam synthetase (BLS) (*38*), carbapenam synthetase (CPS) (*39*), ATP sulfurylase (*40*), ammonia-dependent NAD^+ synthetase (*41*), 4-thiouridine synthetase (*42*), and guanosine-5′-monophosphate synthetase (GMPS) (*43*). With one exception (see below), all enzymes in this family that have been investigated (*34*, *38*, *44*), including AS-B (*8*), do not catalyze the exchange of PP_i into ATP perhaps because PP_i is bound deeply within their synthetase sites when it forms strong, noncovalent interactions with the SGGDXS loop of the common adenylating domain (Figure 6B), which precludes (i) PP_i dissociation until late in the kinetic mechanism and (ii) facile ATP/PP_i exchange. Moreover, on the basis of crystallography and molecular modeling of AS-B (Ding et al., unpublished results) PP_i is likely coordinated to a Mg^{2+} ion that is bound by the conserved aspartate (Asp-238 in AS-B) in the loop motif. We hypothesize that the presence of the metal, and numerous PP_i/loop noncovalent interactions, results in restricted rotation about the P−O bonds, thereby lowering the rate constant associated with PIX to a value that is too low for observation using ^{31}P NMR. In contrast, both ATP/PP_i exchange and a detectable PIX rate have been reported for GMPS (*44*), perhaps reflecting differences in the conformational properties of GMPS when compared with other enzymes that possess this evolutionarily related adenylation domain.

PIX experiments employing the E348D AS-B mutant under identical conditions to those employed with WT AS-B also failed to lead to detectable PIX (Figure 4B). Because ^{18}O isotope transfer shows that this mutant can form the βAspAMP intermediate, this result meant that we could not rule out the possibility that the impaired catalytic turnover of this AS-B mutant relative to WT AS-B (Table 2) resulted from reversible formation of βAspAMP rather than from impaired ammonia attack on the intermediate due to incorrect positioning of the carboxylate side chain as implied by our computational model (Figure 1B). As for WT AS-B, ^{31}P resonances associated with AMP and PP_i were not observed in the NMR spectrum of the reaction mixture (Figure S3; see Supporting Information). Given the intrinsic ATPase activity observed for the E348D AS-B mutant in the absence of aspartate (Figure 2), it appears that this requires the presence of a nitrogen source, which may be necessary to induce the correct conformation for the conversion of ATP into AMP and PP_i.

In the final set of PIX studies, the His_6-tagged E348A AS-B mutant was incubated with aspartate and [β,γ-$^{18}O_6$]ATP **3** (*25*), again in the absence of either glutamine or ammonia. As before, no PIX could be observed from the ^{31}P resonances associated with the ATP present in these reaction mixtures after a period of 3.5 h, a result consistent with the notion that this AS-B mutant cannot catalyze production of the βAspAMP intermediate. Unfortunately, the absence of PIX also means that βAspAMP may be formed reversibly although the simplest hypothesis remains that the E348A AS-B mutant cannot

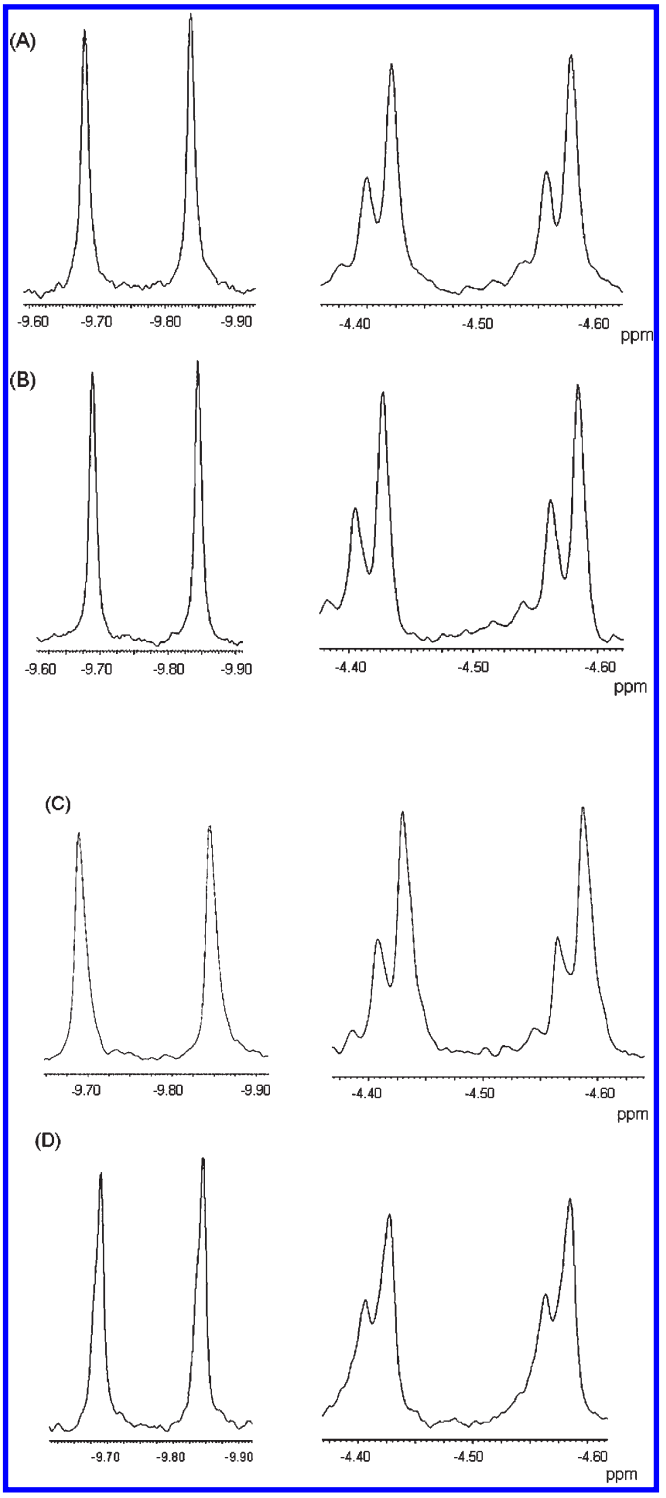

FIGURE 4: ^{31}P NMR spectra of signals associated with the α-P (left) and γ-P (right) in ATP isolated from PIX reaction mixtures containing (A) no enzyme, (B) WT AS-B, (C) the E348D AS-B mutant, and (D) the E348A AS-B mutant after incubation for 3.5 h at 37 °C. No NMR detectable amounts of either AMP or PP_i were produced under these conditions. ^{31}P chemical shifts are referenced to 85% phosphoric acid.

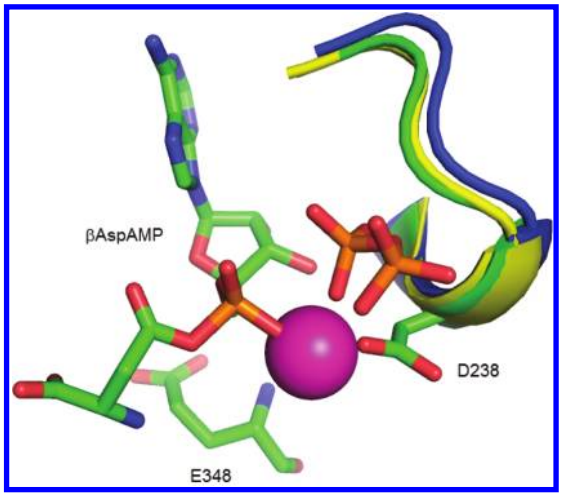

FIGURE 5: Structural overlay of the "P-loop" in the adenylating domains of AS-B (green), argininosuccinate synthetase (yellow), and BLS (blue) together with the βAspAMP intermediate, $MgPP_i$, and the functionally important residues Asp-238 and Glu-348 in a computational model of the AS-B/glutamine/βAspAMP/$MgPP_i$ complex (Ding and Richards, unpublished results). βAspAMP, PP_i, Asp-238, and Glu-348 are shown in stick representations, and the Mg(II) ion is rendered as a magenta sphere. Atom coloring: C, gray; H, white; O, red; N, blue; P, orange. Image rendered in PYMOL.

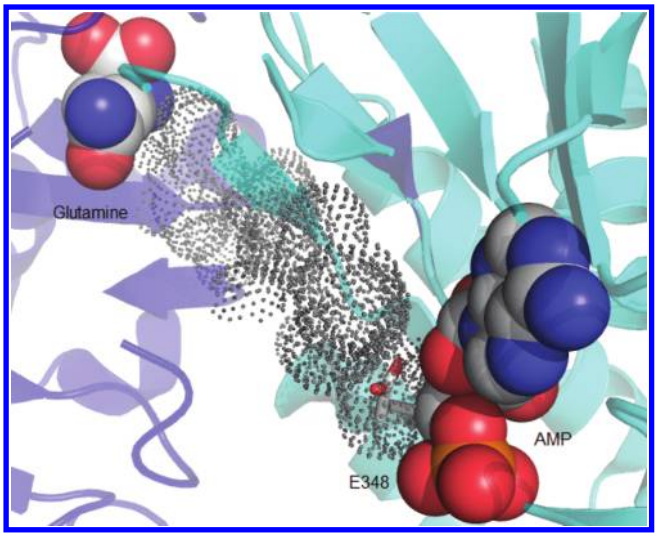

FIGURE 6: View of the intramolecular tunnel (black dots) in the *E. coli* AS-B C1A/glutamine/AMP complex (1CT9) showing the location of the Glu-348 (E348) side chain relative to the tunnel connecting the two active sites. The cartoon representations of the glutaminase and synthase domains of the C1A AS-B mutant are colored blue and cyan, respectively. Glutamine and AMP are rendered as CPK models while Glu-348 is shown in a stick representation. Coloring: C, gray; O, red; N, blue; P, orange. The image was rendered in PYMOL.

catalyze formation of this intermediate, thereby precluding asparagine production. More direct ^{31}P NMR-based methods of detecting enzyme-bound βAspAMP appear to be ruled out by the size of the enzyme, which is active in solution as a dimer (Li et al., unpublished observations). As in the other two PIX studies, no ^{31}P resonances associated with AMP and PP_i were observed (Figure S4; see Supporting Information), although the very low intrinsic ATPase activity (Figure 2) might have produced insufficient amounts of these products for detection in our spectra. It remains possible, however, that ATP breakdown cannot take place in the absence of a nitrogen source.

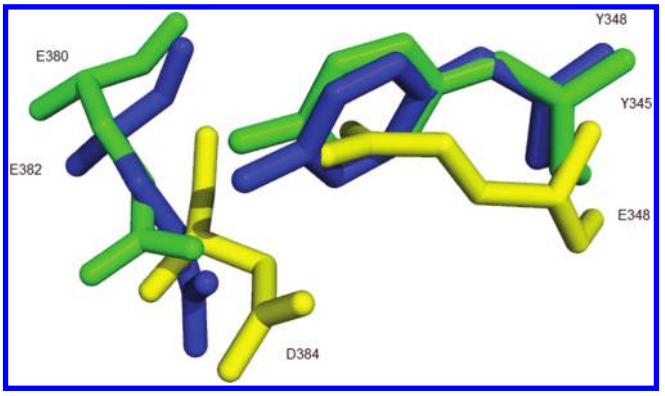

FIGURE 7: Structural overlay of the "catalytic dyad" residues that are conserved in BLS (Tyr-348 and Glu-382, blue) and CPS (Tyr-345 and Glu-380, green) with the corresponding residues (Glu-348 and Asp-384) in the AS-B synthetase site of AS-B. The image was rendered in PYMOL.

Scheme 4: Kinetic Model for the Glutaminase and Synthetase Reactions Catalyzed by AS-B[a]

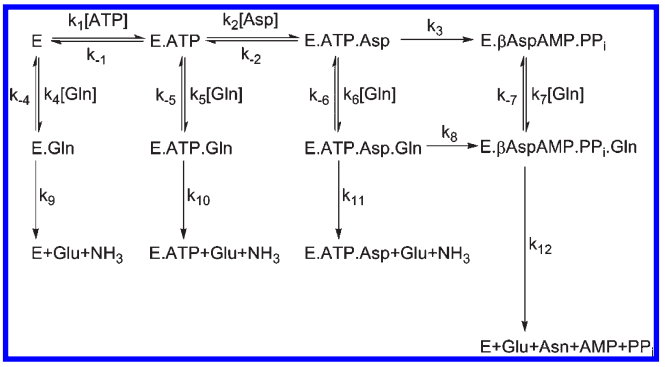

[a]Reprinted from ref *18* with permission from Elsevier.

CONCLUSIONS

Taken overall, these experiments clearly demonstrate that Glu-348 has an important functional role in catalysis. Although it is possible that this residue does participate as a general base during the reaction of ammonia with βAspAMP, our experiments show that the negatively charged side chain is somehow essential for reaction of ATP with bound aspartate to form the adenylated intermediate. Substantial proof for this assertion is provided by the ^{18}O-transfer experiments on the E348A and E348D AS-B mutants. Such a hypothesis is also consistent with the altered Glu:Asn stoichiometry exhibited by WT AS-B and the E348D AS-B mutant. This can be seen by considering the kinetic scheme for the substrate binding steps in AS-B (Scheme 4) (*18*). In this proposal, glutamine hydrolysis takes place even in the presence of saturating concentrations of ATP and aspartate because the rate constants of glutamine binding to the E·Asp·ATP complex (k_6) and subsequent hydrolysis (k_{11}) are similar to the rate of βAspAMP formation (k_3 or k_8). In the case of the E348D AS-B mutant, the observed rate of asparagine production is halved, presumably because of a decrease in the rate constant for βAspAMP formation (k_3 or k_8) that is similar in magnitude. Thus, more glutamine is hydrolyzed per asparagine in the E348D AS-B mutant because the steady-state concentration of the E·ATP·Asp·Gln complex is increased for the mutant enzyme relative to WT AS-B under identical conditions. Of course, this might also be the case if attack of ammonia on the intermediate were significantly impaired by the loss of the Glu-348 side chain

Scheme 5: Reactions Catalyzed by (A) BLS and (B) CPS Showing the Similarity of Chemical Mechanisms of These Enzymes to That of Glutamine-Dependent ASNS

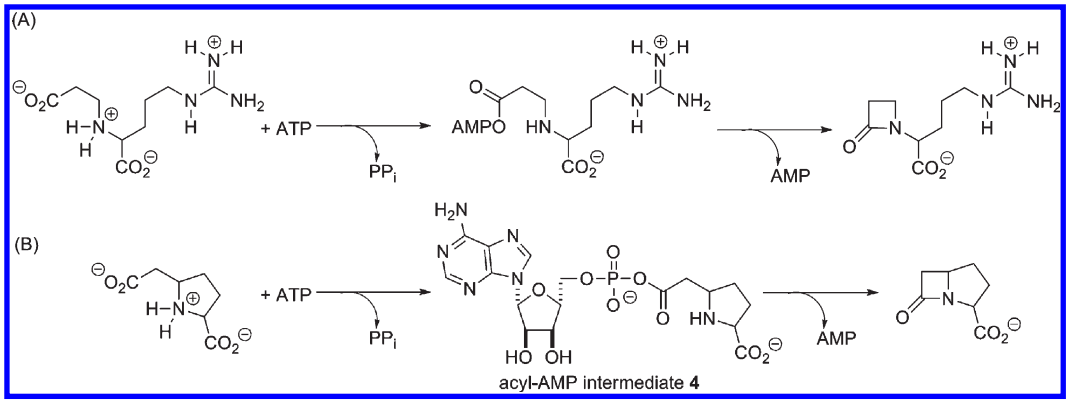

acting as a general base, leading to reversible βAspAMP formation and leakage of ammonia from the enzyme. In this case, the very low rate of PIX ($< 0.003\ s^{-1}$) might then result from a lack of pyrophosphate rotation due to strong complexation by Mg^{2+}. A third explanation for the increased decoupling of the glutaminase and synthetase activities in the E348D AS-B mutant is that changing the length of the negatively charged side chain impairs the adoption of a conformation that is necessary for the efficient translocation of ammonia between the two active sites. In this case, it can be imagined that the tunnel is more solvent exposed in the E348D AS-B mutant leading to loss of ammonia because of an impaired rate of βAspAMP formation.

Whichever of these arguments is correct, Glu-348 also seems to participate in the molecular mechanisms that couple the glutaminase and synthetase activities, albeit to a smaller extent than observed for other glutamine-dependent amidotransferases (*45*). Thus, when ATP is present, the k_{cat}/K_m for glutamine in the glutaminase reaction increases 6-fold for the E348D AS-B mutant compared to only a 2-fold increase for the wild-type enzyme. Removal of the side chain effectively eliminates the ATP dependence of glutaminase activity (Table 1). On this point, we note that the negatively charged side chain of Glu-348 is located at the C-terminal end of the ammonia tunnel linking the active sites (Figure 6) and may be involved in interactions that facilitate ammonia transfer, perhaps in a manner similar to those observed in computational studies on glutamine fructose-6-phosphate amidotransferase (*46*, *47*).

Our observations of the functional properties of Glu-348 are given added interest by the observation that the tyrosine residue located in the cognate position in the synthetase sites of BLS (Tyr-348) and CPS (Tyr-345) has been shown to participate in acid/base catalysis leading to formation of a β-lactam from an acyl-AMP intermediate (Scheme 4) (*48*). As might have been expected from the chemical similarity of the reactions catalyzed by all three enzymes, evidence from crystallography (*39*, *49*, *50*) and sequence alignment studies (*51*) is consistent with the hypothesis that BLS and CPS, which are involved in secondary metabolite biosynthesis, both evolved from ASNS. Structural overlay clearly shows that Tyr-348, Tyr-345, and Glu-348 all occupy identical locations in the three synthetase sites (Figure 7). In contrast to our observation that mutation of Glu-348 impairs acyl-adenylate formation, replacement of Tyr-345 in CPS by alanine yields a mutant in which β-lactam ring formation is impaired, leading to reversible formation of acyl-AMP **4** (Scheme 5) and the appearance of ATP/PP_i exchange (*48*). Thus, the Y345A CPS mutant can catalyze the adenylation reaction but lacks the ability to control the proton transfer steps that result in irreversible β-lactam ring formation. In light of this result, it remains possible that Glu-348 can participate as a general base to facilitate the attack of ammonia on βAspAMP. If this is the case, then the decreased rate of βAspAMP formation in the E348D AS-B, and the inability of the E348A and E348Q mutants to adenylate aspartate, may arise from the lack of a large forward commitment for asparagine production. The differences in the ability of the E348A AS-B and Y345A CPS mutants to form the adenylate derivatives of their respective substrates demonstrate the difficulty of predicting subtle differences in active site properties for enzymes that share a common ancestor and catalyze essentially identical chemical reactions.

ACKNOWLEDGMENT

We thank Dr. LaKenya Williams for synthesizing the sample of [β,γ-$^{18}O_6$]ATP that was used in the PIX experiments.

SUPPORTING INFORMATION AVAILABLE

Figures S1−S4 as described in the text. This material is available free of charge via the Internet at http://pubs.acs.org.

REFERENCES

1. Richards, N. G. J., and Schuster, S. M. (1998) Mechanistic issues in asparagine synthetase catalysis. *Adv. Enzymol. Relat. Areas Mol. Biol. 72*, 145–198.
2. Lorenzi, P. L., Llamas, J., Gunsior, M., Ozbun, L., Reinhold, W. C., Varma, S., Ji, H., Kim, H., Hutchinson, A. A., Kohn, E. C., Goldsmith, P. K., Birrer, M. J., and Weinstein, J. N. (2008) Asparagine synthetase is a predictive biomarker of L-asparaginase activity in ovarian cancer cell lines. *Mol. Cancer Ther. 7*, 3123–3128.
3. Lorenzi, P. L, Reinhold, W. C., Rudelius, M., Gunsior, M., Shankavaram, U., Bussey, K. J., Scherf, U., Eichlerl, G. S., Martin, S. E., Chin, K., Gray, J. W., Kohn, E. C., Horak, I. D., Von Hoff., D. D., Raffeld, M., Goldsmith, P. K., Caplen, N. J., and Weinstein, J. N. (2006) Asparagine synthetase as a causal, predictive biomarker for L-asparaginase activity in ovarian cancer cells. *Mol. Cancer Ther. 5*, 2613–2623.
4. Aslanian, A. M., Fletcher, B. S., and Kilberg, M. S. (2001) Asparagine synthetase expression alone is sufficient to induce L-asparaginase resistance in MOLT-4 human leukaemia cells. *Biochem. J. 357*, 321–328.
5. Richards, N. G. J., and Kilberg, M. S. (2006) Asparagine synthetase chemotherapy. *Annu. Rev. Biochem. 75*, 629–654.
6. Gutierrez, J. A., Pan, Y.-X., Koroniak, L., Hiratake, J., Kilberg, M. S., and Richards, N. G. J. (2006) An inhibitor of human asparagine synthetase suppresses proliferation of an L-asparaginase-resistant leukemia cell line. *Chem. Biol. 13*, 1339–1347.
7. Ciustea, M., Gutierrez, J. A., Abbatiello, S. E., Eyler, J. R., and Richards, N. G. J. (2005) Efficient expression, purification, and characterization of C-terminally tagged, recombinant human asparagine synthetase. *Arch. Biochem. Biophys. 440*, 18–27.

8. Boehlein, S. K., Stewart, J. D., Walworth, E. S., Thirumoorthy, R., Richards, N. G. J., and Schuster, S. M. (1998) Kinetic mechanism of *Escherichia coli* asparagine synthetase B. *Biochemistry 37*, 13230–13238.
9. Boehlein, S. K., Walworth, E. S., Richards, N. G., and Schuster, S. M. (1997) Mutagenesis and chemical rescue indicate residues involved in β-aspartyl-AMP formation by *Escherichia coli* asparagine synthetase B. *J. Biol. Chem. 272*, 12384–12392.
10. Boehlein, S. K., Richards, N. G., Walworth, E. S., and Schuster, S. M. (1994) Arginine 30 and asparagine 74 have functional roles in the glutamine dependent activities of *Escherichia coli* asparagine synthetase B. *J. Biol. Chem. 269*, 26789–26795.
11. Boehlein, S. K., Walworth, E. S., and Schuster, S. M. (1997) Identification of cysteine-523 in the aspartate binding site of *Escherichia coli* asparagine synthetase B. *Biochemistry 36*, 10168–10177.
12. Blundell, T. L., Jhoti, H., and Abell, C. (2002) High-throughput crystallography for lead discovery in drug design. *Nat. Rev. Drug Discov. 1*, 45–54.
13. Boehlein, S. K., Nakatsu, T., Hiratake, J., Thirumoorthy, R., Stewart, J. D., Richards, N. G. J., and Schuster, S. M. (2001) Characterization of inhibitors acting at the synthetase site of *Escherichia coli* asparagine synthetase B. *Biochemistry 40*, 11168–11175.
14. Larsen, T. M., Boehlein, S. K., Schuster, S. M., Richards, N. G., Thoden, J. B., Holden, H. M., and Rayment, I. (1999) Three-dimensional structure of *Escherichia coli* asparagine synthetase B: a short journey from substrate to product. *Biochemistry 38*, 16146–16157.
15. Petrey, D., and Honig, B. (2005) Protein structure prediction: inroads into biology. *Mol. Cell 20*, 811–819.
16. Arnold, K., Bordoli, L., Kopp, J., and Schwede, T. (2006) The SWISS-MODEL workspace: a web-based environment for protein structure homology modelling. *Bioinformatics 22*, 195–201.
17. Ikeuchi, H., Meyer, M. E., Ding, Y., Hiratake, J., and Richards, N. G. J. (2009) A critical electrostatic interaction mediates inhibitor recognition by human asparagine synthetase. *Bioorg. Med. Chem. 17*, 6641–6650.
18. Tesson, A. R., Soper, T. S., Ciustea, M., and Richards, N. G. J. (2003) Revisiting the steady state kinetic mechanism of glutamine-dependent asparagine synthetase from *Escherichia coli*. *Arch. Biochem. Biophys. 413*, 23–31.
19. Koroniak, L., Ciustea, M., Gutierrez, J. A., and Richards, N. G. J. (2003) Synthesis and characterization of an N-acylsulfonamide inhibitor of human asparagine synthetase. *Org. Lett. 5*, 2033–2036.
20. Bradford, M. M. (1976) A rapid and sensitive method for the quantitation of microgram quantities of protein utilizing the principle of protein-dye binding. *Anal. Biochem. 72*, 248–254.
21. Thompson, J. S., and Edmonds, O. P. (1980) Safety aspects of handling the potent allergen FDNB. *Ann. Occup. Hyg. 23*, 27–33.
22. Boehlein, S., Richards, N., and Schuster, S. (1994) Glutamine-dependent nitrogen transfer in *Escherichia coli* asparagine synthetase B. *J. Biol. Chem. 269*, 7450–7457.
23. Cleland, W. W. (1979) Statistical analysis of enzyme kinetic data. *Methods Enzymol. 62*, 151–160.
24. Li, K. K., Beeson, W. T., Ghiviriga, I., and Richards, N. G. J. (2007) A convenient gHMQC-based NMR assay for investigating ammonia channeling in glutamine-dependent amidotransferases: studies of *Escherichia coli* asparagine synthetase B. *Biochemistry 46*, 4840–4849.
25. Williams, L., Fan, F., Blanchard, J. S., and Raushel, F. M. (2008) Positional isotope exchange analysis of the *Mycobacterium smegmatis* cysteine ligase (MshC). *Biochemistry 47*, 4843–4850.
26. Cohn, M., and Hu, A. (1980) Isotopic oxygen-18 shifts in phosphorus-31 NMR of adenine nucleotides synthesized with oxygen-18 in various positions. *J. Am. Chem. Soc. 102*, 913–916.
27. Luehr, C. A., and Schuster, S. M. (1985) Purification and characterization of beef pancreatic asparagine synthetase. *Arch. Biochem. Biophys. 237*, 335–346.
28. Raushel, F. M., and Villafranca, J. J. (1988) Positional isotope exchange. *CRC Crit. Rev. Biochem. 23*, 1–26.
29. Sheng, S., Moraga-Amador, D. A., van Heeke, G., Allison, R. D., Richards, N. G. J., and Schuster, S. M. (1993) Glutamine inhibits the ammonia-dependent activities of two Cys-1 mutants of human asparagine synthetase through the formation of an abortive complex. *J. Biol. Chem. 268*, 16771–16780.
30. Sheng, S., and Schuster, S. M. (1993) Purification and characterization of *Saccharomyces cerevisiae* DNA damage-responsive protein 48 (DDRP 48). *J. Biol. Chem. 268*, 4752–4758.
31. Boehlein, S. K., Walworth, E. S., Richards, N. G. J., and Schuster, S. M. (1997) Mutagenesis and chemical rescue indicate residues involved in β-aspartyl-AMP formation by *Escherichia coli* asparagine synthetase B. *J. Biol. Chem. 272*, 12384–12392.
32. Villafranca, J. J. (1989) Positional isotope exchange using phosphorus-31 nuclear magnetic resonance. *Methods Enzymol. 177*, 390–403.
33. Rognes, S. E. (1975) Glutamine-dependent asparagine synthetase from *Lupinus luteus*. *Phytochemistry 14*, 1975–1982.
34. Hilscher, L. W., Hanson, C. D., Russell, D. H., and Raushel, F. M. (1985) Measurement of positional isotope exchange rates in enzyme-catalyzed reactions by fast atom bombardment mass spectrometry: application to argininosuccinate synthetase. *Biochemistry 24*, 5888–5893.
35. Ghose, C., and Raushel, F. M. (1985) Determination of the mechanism of the argininosuccinate synthetase reaction by static and dynamic quench experiments. *Biochemistry 24*, 5894–5898.
36. Goto, M., Omi, R., Miyahara, I., Sugahara, M., and Hirotsu, K. (2003) Structures of argininosuccinate synthetase in enzyme-ATP substrates and enzyme-AMP product forms. *J. Biol. Chem. 278*, 22964–22971.
37. Bork, P., and Koonin, E. V. (1994) A P-loop-like motif in a widespread ATP pyrophosphatase domain: implications for the evolution of sequence motifs and enzyme activity. *Proteins: Struct., Funct., Genet. 20*, 347–355.
38. Bachmann, B. O., and Townsend, C. A. (2000) Kinetic mechanism of the β-lactam synthetase of *Streptomyces clavuligerous*. *Biochemistry 39*, 11187–11193.
39. Miller, M. T., Gerratana, B., Stapon, A., Townsend, C. A., and Rosenzweig, A. C. (2003) Crystal structure of carbapenam synthetase (CarA). *J. Biol. Chem. 278*, 40996–41002.
40. Mougous, J. D., Lee, D. H., Hubbard, S. C., Schelle, M. W., Vocadlo, D. J., Berger, J. M., and Bertozzi, C. R. (2006) Molecular basis for G protein control of the prokaryotic ATP sulfurylase. *Mol. Cell 21*, 109–122.
41. Rizzi, M., Bolognesi, M., and Coda, A. (1998) A novel deamido-NAD(+)-binding site revealed by the trapped NAD-adenylate intermediate in the NAD(+) synthetase structure. *Structure 6*, 1129–1140.
42. Waterman, D. G., Ortiz-Lombardi, M., Fogg, M. J., Koonin, E. V., and Antson, A. A. (2006) Crystal structure of *Bacillus anthracis* ThiI, a tRNA-modifying enzyme containing the predicted RNA-binding THUMP domain. *J. Mol. Biol. 356*, 97–110.
43. Tesmer, J. G., Klem, T. J., Deras, M. L., Davisson, V. J., and Smith, J. L. (1996) The crystal structure of GMP synthetase reveals a novel catalytic triad and is a structural paradigm for two enzyme families. *Nat. Struct. Biol. 3*, 74–86.
44. Von der Saal, W., Crysler, C. S., and Villafranca, J. J. (1985) Positional isotope exchange and kinetic experiments with *Escherichia coli* guanosine 5′-monophosphate synthetase. *Biochemistry 24*, 5343–5350.
45. Richards, N. G. J., Humkey, R. N., Li., K., Meyer, M. E., and Sintjago de Cordova, T. C. (2010) Tunnel and intermediates in the glutamine-dependent amidotransferases, in Comprehensive Natural Products II: Chemistry & Biology (Mander, L., and Liu, H.-W., Eds.) Vol. 8, pp 161−230, Elsevier, Oxford.
46. Floquet, N., Durand, P., Maigret, B., Badet, B., Badet-Denisot, M.-A., and Perahia, D. (2009) Collective motions in glucosamine-6-phosphate synthase: influence of ligand binding and role in ammonia channeling and opening of the fructose-6-phosphate binding site. *J. Mol. Biol. 385*, 653–664.
47. Mouilleron, S., Badet-Denisot, M.-A., and Golinelli-Pimpaneau, B. (2008) Ordering of C-terminal loop and glutaminase domains of glucosamine-6-phosphate synthase promotes sugar ring opening and formation of the ammonia channel. *J. Mol. Biol. 377*, 1174–1185.
48. Raber, M. L., Arnett, S. O., and Townsend, C. A. (2009) A conserved tyrosyl-glutamyl catalytic dyad in evolutionarily linked enzymes: carbapenem synthetase and β-lactam synthetase. *Biochemistry 48*, 4959–4971.
49. Miller, M. T., Bachmann, B. O., Townsend, C. A., and Rosenzweig, A. C. (2002) The catalytic cycle of β-lactam synthetase observed by x-ray crystallographic snapshots. *Proc. Natl. Acad. Sci. U.S.A. 99*, 14752–14757.
50. Miller, M. T., Bachmann, B. O., Townsend, C. A., and Rosenzweig, A. C. (2001) Structure of β-lactam synthetase shows how to synthesize antibiotics instead of asparagine. *Nat. Struct. Biol. 8*, 684–689.
51. Bachmann, B. O., Li, R., and Townsend, C. A. (1998) β-Lactam synthetase: a new biosynthetic enzyme. *Proc. Natl. Acad. Sci. U.S.A. 95*, 9082–9086.